Structural Energy Distribution and Particle Phase Stability Study of Longitudinal Dynamics of a Simple Linear Proton Accelerator

R. Timalsina

Journal of Nepal Physical Society

Volume 7, Issue 1, April 2021

(Special Issue: ANPA Conference, 2020)

ISSN: 2392-473X (Print), 2738-9537 (Online)

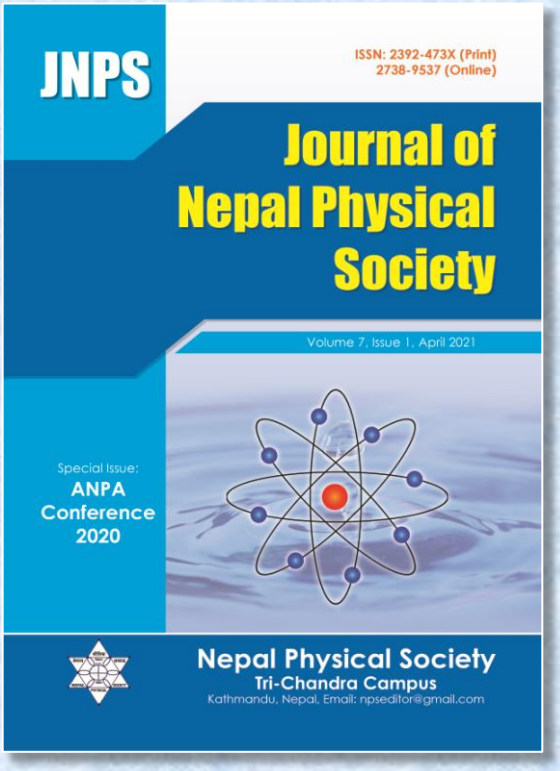

JNPS, **7** (1), 66-72 (2021)

DOI: http://doi.org/10.3126/jnphyssoc.v7i1.36978

Published by:

Nepal Physical Society

P.O. Box: 2934

Tri-Chandra Campus

Kathmandu, Nepal

Email: npseditor@gmail.com

JNPS 7 (1): 66-72 (2021)
ISSN: 2392-473X (Print), 2738-9537 (Online)

Research Article *© Nepal Physical Society*
DOI: http://doi.org/10.3126/jnphyssoc.v7i1.36978

Structural Energy Distribution and Particle Phase Stability Study of Longitudinal Dynamics of a Simple Linear Proton Accelerator

R. Timalsina
Tribhuvan University, Kathmandu, Nepal
Corresponding Email: rasminsharma111@gmail.com

Received: *10 August, 2020;* ***Revised:*** *16 March, 2021;* ***Accepted:*** *24 March, 2021*

ABSTRACT

This paper presents the study of longitudinal beam dynamics of a simple linear proton accelerator and simulation results for a model linear accelerator (LINAC) using MATLAB. The study part of the transition energy, particle acceleration, transit time factor, RF factor, and momentum compaction are discussed. For the simulation, the model LINAC is built using unit cells and the unit cell consists of Quadrupole doublet and acceleration cavity. Model LINAC's basic setup is present and the simulation is based on the single-particle analysis. The robustness of the model LINAC tested to operate varying different parameters like initial arrival phase and input energy. The criteria to measure the robustness of the model LINAC are to check the kinetic energy at the end of the LINAC and the transverse stability of the transfer matrices of each cell. The paper also presents the theoretical analysis of phase stability at both below and above transition energy. The stability of small and larger amplitude oscillations are present and simulation results for different particles each starting with different amplitudes observed, where the large amplitude oscillation falls outside of the separatrix.

Keywords: Radio Frequency Factor; Linear Accelerator; Electromagnetic; High Energy Physics.

1. INTRODUCTION

A particle accelerator is an apparatus used in physics research devoted to high-energy physics with nature of physical universe to produce a beam of energetic charged particles at high speed directed against various targets. These use the EM field to accelerate and steer particles. RF cavities boost the particle beams, while magnets focus the beam and bend their trajectory. The invention of the linear accelerator, betatron, cyclotron, synchrotron, and storage ring are with an extended based program including different strategies [1]. LINAC accelerates charged subatomic particles to an exorbitant speed by vanquishing them to a series of oscillating electric potentials along a linear beamline. A large number of particles are injected and accelerated each cycle for the production of higher energies and accelerate heavy ions [2]. The principles LINAC were contemplated by Gustav Ising in 1924 while the first machine that worked was constructed by Rolf Widerøe in 1928 at the RWTH Aachen University, brought about X-rays and high energy electrons for radiation therapy assist as particle injectors for higher-energy accelerators [3]. The application purpose of LINAC is in industry, medicine, and research and use as a beamer and waveguide for protons. We have focused on the interaction of transverse electrical and magnetic fields with charged particles and have studied appropriate formalism to apply this interaction to the design of beam transport systems. By using the concept related to beam size, magnet construction, RF measurements are explored including subsystems of Ziemann [4] we tried to study and analyze the mathematical simulation of LINAC. Encountering the instability of particle motion and the beam size verification, are generalized in this study.

The outline of the paper is as follows: In Sec. 2, we discuss the methods of analysis, where theoretical and mathematical calculation of LINAC is illustrated, and computational details accompanied

by MATLAB® code of our work are stated in particular. Then using various data and parameters, results of work are presented in Sec. 3 and the conclusions are collected in Sec. 4.

2. METHODOLOGY

2.1 Theoretical Background

2.1.1 Longitudinal Oscillations

We consider the methods of system which electrical fields to transfer energy to the beam. EM fields in the RF range are used to reach higher energies. If the accelerator is circular, we use individual accelerating gaps and they are typically located in resonant structures. The acceleration cavities play such a central role in charged particle accelerators which further proceed with a simple prototype. The pill-box cavity in a precise way and analyze the EM fields that can oscillate inside the cavity. The dynamics of the EM fields is governed by Maxwell's equations in vacuum with no charges or currents present.

Calculation of transverse field components from longitudinal field components are:

$H_z = \frac{i\omega\varepsilon}{{k_c}^2}\frac{\partial E_z}{\partial y}$, $H_y = \frac{-i\omega\varepsilon}{{k_c}^2}\frac{\partial E_z}{\partial x}$, $E_z = \frac{-iK_z}{{k_c}^2}\frac{\partial E_z}{\partial x}$,

$E_y = \frac{-iK_z}{{k_c}^2}\frac{\partial E_z}{\partial y}$, where ${k_c}^2 = \frac{\omega^2}{c^2} - {K_z}^2$

The solution [4] for the longitudinal electric field component represent as $E_z(r,\phi,z,t) = E_0 J_m(k_c r)e^{\pm im\phi}e^{\pm iK_z z}e^{i\omega t}$. The dispersion relation for the resonance frequencies is given by $\frac{{\omega_{mnp}}^2}{c^2} = \left(\frac{\gamma_{mn}}{R}\right)^2\left(\frac{p\pi}{l}\right)^2$, where γ is twiss-parameter (kinetic factor), *m*, *n* and *p* are an integer, $r = R$ is radius, *l* = length of the cavity, λ is wavelength, and admissible frequencies are $f_{mnp} = \frac{\omega_{mnp}}{2\pi}$. We have, $R = \frac{2.405\lambda}{2\pi\sqrt{1-(\frac{p\lambda}{2l})^2}} = 0.23m$, for $m, p = 0$ and $n = 1$.

Hence, TM_{101}-mode has a non-zero longitudinal field component E_z and is used to accelerate the particle. It excites the beam which leads to instability. The generation of RF power needs to excite the field cavity and for maximum acceleration voltage, all the time during its traversal of the cavity observed by the transit-time factor [5]. Transit time factor T(*x*) characterizes the energy gain of a particle passing through an acceleration gap which gives energy change. The energy gain ΔW of a particle with charge q that arrives in the center of the cavity with phase ϕ is given by [4]

$$\Delta W = qE_z l\cos(\phi)\frac{\sin(\frac{\omega_{rf}l}{2\beta c})}{\frac{\omega_{rf}l}{2\beta c}} \quad (1)$$

with $T(z) = \frac{z}{\beta c}$, where βc is the velocity of the particle and E_z is the peak longitudinal electric field in the pill-box cavity. The energy gain by the particle had been received during the traversal, had it been exposed to the peak field the whole time. Since, the field varies during the traversal, it is reduced by the transit time factor $T(x) = \frac{\sin(x)}{x}$ with $x = \frac{\omega_{rf}l}{2\beta c}$.

Phase stability and Synchrotron Oscillation:

Here, $\ddot{\psi} + \Omega_s\psi = 0$ with ${\Omega_s}^2 = \frac{-\omega_{rfn}\cos\phi_s}{T_0\beta^2}\frac{e\hat{V}}{E}$ is the differential equation for a harmonic oscillator and describes oscillations with the synchrotron frequencies where design-phase motion is stable and particles perform stable oscillation [6]. The synchronous phase ϕ_s of the RF-cavity at which the reference particle should arrive is determined by external requirements, such as to achieve maximum acceleration, which is indicated by the particle located at the crest of the oscillation [4]. The energy U_d delivered to the beam in every turn and this needs to be provided by the accelerating cavity. The synchronous phase ϕ_s at which the beam receives this energy is then given by

$$U_d = qV\sin(\phi_s).$$

Here the dynamics of a particle in longitudinal phase space is described as follows [3]

$$\frac{d\delta}{dt} = \frac{1}{T_0\beta}\frac{\Delta E}{E} = \frac{e\hat{V}}{T_0\beta E}[\sin\phi - \sin\phi_s] \quad (2)$$

$$\frac{d\phi}{dt} \simeq \omega_{rf}\frac{d\tau}{T_0} = \omega_{rfn}\delta - \omega_{rf\alpha}\frac{\alpha B}{B} \quad (3)$$

Large-Amplitude Oscillation:

When injecting new particles into a ring, normally energy and phase of the new particles should be adjusted to arrive near the point where stable oscillation occurs [6]. The equation of mathematical pendulum implemented for fixing unit and space oscillation to simplify assumption $\phi_s = 0$ is large oscillation, $\ddot{\phi} + {\Omega_s}^2\sin\phi = 0$. For the bucket half-height, maximum momentum acceptance of phase slip factor (η), $\delta_{max} = 2\sqrt{\frac{1}{\eta\omega_{rf}\beta^2 T_0}\frac{e\hat{V}}{E}}$. Similarly, the oscillation period, $T_p = T_s\left(\frac{2}{\pi}\right)K\sin\left(\frac{\hat{\phi}}{2}\right)$. Using Jacobi elliptic function for small-amplitude

oscillation, the separatrix structure in the form of an equation is represented by

$$sin\left(\frac{\phi}{2}\right) = Ksn(\Omega_s t + f(z_0, K,), K)$$

$$\dot{\phi} = 2\Omega_s K cn(\Omega_s t + f(z_0, K,), K) \quad (4)$$

This equation is the main formula used for the pendulum tracker revealed for perturbation act of EM field as a function [5].

2.1.2 Acceleration

For the process of acceleration, the RF system has to continuously transfer energy to particles based on U_d that design phase ϕ_s has to be different from 0 to π. It describes the measured variations of field dipole with ring size. So that, ramping the dipole field is given by $\frac{\Delta B}{B} = \frac{\rho \dot{\beta} t}{\beta \frac{E}{c}}$ and effective potential is $V_{eff}(\phi)$= -$\hat{\Omega}_s^{\,2}$ $(cos\phi + \phi sin\phi_s)$. The conservation of energy for the dynamic of a particle is given by $\frac{dA}{dt} = 0$ where, A = $[\frac{1}{2}\dot{\phi}^2 - \hat{\Omega}_s^{\,2}(cos\phi + \phi sin\phi_s)]$ is constant. Hence, the maximum of separatrix defines by $\dot{\phi}$ is represented as,

$$\dot{\phi} = \pm\hat{\Omega}_s\sqrt{2(cos\phi + cos\phi_s - [(2n+1)\pi - \phi - \phi_s]sin\phi_s)}.$$

Here, maximum acceleration is observed by increasing synchronous phase angle ϕ_s [3]. In RF gymnastics, equivalent Hamiltonian system describes the mathematical pendulum where the Hamiltonian system remains constant in adiabatic invariant, since, $\frac{d\Omega_s}{dt} \ll \Omega_s^2$, creates longitudinal emittance constant. Length and $\hat{V}$ of the RF system with an experiment leads to bunch rotation, de-bunching re-bunching, bunch splitting, and batch compression [7]. Hence, the RF system analyses the longitudinal motion of particles at fixed energy of about MeV range.

2.1.3 Simple LINAC Model

For the simple linear proton accelerator, the beam enters from the left with energy γ_0 and passes through several cells, length $L = 30$, each made of one cavity with the design phase ψ_i, maximum energy gain g_i, and a quadrupole doublet to provide transverse focusing. The equations that govern the dynamics in the longitudinal phase space are [4]

$$\gamma_{i+1} = \gamma_i + g_i sin(\phi_i - \psi_i) \text{ and} \quad 5(a)$$

$$\phi_{i+1} = \phi_i + \frac{\frac{\omega L}{c}}{\sqrt{1-\frac{1}{\gamma_i^2}}} \quad 5(b)$$

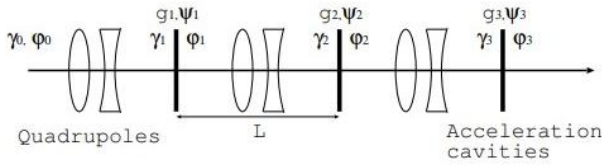

Fig. 2.1.3: Simple Linear Proton Accelerator

The first equation describes the energy added to the particle in the cavity where g_i is in the unit of particles rest mass. The energy gain depends on the design phase ψ_i of that cavity and the actual arrival phase ϕ_i of the particle. The second equation describes the change in arrival phase that depends on the distance L between the cavities, the speed of the particle v_i, and the frequency ω of the cavity.

2.2 Computational Approach

The computer software MATLAB/Simulink R2016a is used to figure out all the simulation of the mathematical calculation and plot the representation of LINAC. The method first starts by including step by step script (MATLAB® program) which plot and label the given data and command, and end the system calculation with the proper format in the graphical process. For the script, the file should be saved like name.m form, then define the parameters and run the saved file. This scripted file contains different functions having one or more inputs and results in an output.

3. RESULTS AND DISCUSSION

3.1 Acceleration

The schematic representation of the longitudinal potential for the two synchronous phase angles shown below in figure 3.1.1 where, the upper plot of (a) displays V_{eff} and the separatrices in the lower plot. The stable phase region shown on plot (b) which is produced by the first half of the script for smaller buckets. Here, maximum of separatrix defines by $\dot{\Phi}$ is represented as,

$$\dot{\Phi} = \pm\hat{\Omega}_s\sqrt{2(\cos\Phi + \cos\Phi_s - [(2n+1)\pi - \Phi - \Phi_s]\sin\Phi_s}$$

The ranges of the expression under the root that is $\dot{\phi}$ is positive. Plot (c) is produced by the lower part of the script of the smaller bucket. The height of the separatrix is maximum above the stable phase ϕ_s and plotted as function of ϕ_s by defining the bucket-half-height. Hence, the range of phases and the momentum acceptance is

reduced at increasing synchronous phase angle ϕ_s and operating at maximum acceleration with ϕ_s= 90 degrees, is only marginally feasible, because the stable region of synchrotron oscillations shrinks to a single point and stability of longitudinal motion is lost.

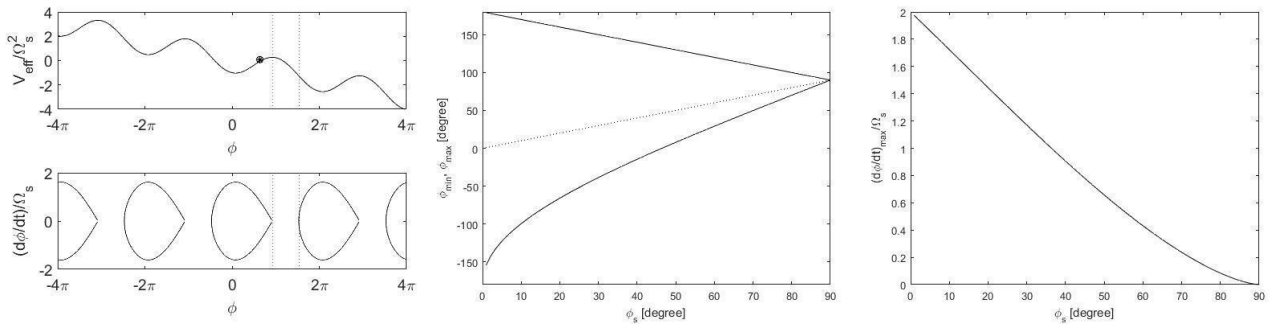

Fig. 3.1.1: Graph (a) shows effective potential V_{eff} for the asynchronous phase of $\phi_s = 14$ degrees (solid) and $\phi_s = 75$ degrees (dashed). Here, bottom plot shows corresponding regions where stable oscillations are possible (Longitudinal potential). Graphs (b) and (c) represent the stable phase region and bucket half-height as a function of the synchronous phase respectively.

3.2 Longitudinal Oscillation

The phase portrait of the motion in the longitudinal phase space is generated by script for separatrix. It is based on equation $\dot{\phi} = \Omega_s\sqrt{2(cos\phi - cos\hat{\phi})}$. Separatrix shown on the plot (a) where axes are annotated with multiples of $\frac{\pi}{2}$. Large oscillation period as a function of maximum amplitude $\hat{\phi}$ shown on plot (b) which is produced by following script related to oscillation period and it is straight implementation of t_p. Here, t_p is the function of t_s. The trajectories with six different starting amplitudes are based on the integration routine for the mathematical pendulum called pendulum tracker. It is based on the $\dot{\phi} = \pm 2\Omega_s K dn\left(\Omega_s K t + f\left(\frac{\Phi_0}{2}, \frac{1}{K}\right), \frac{1}{K}\right)$, depending on whether the variable K is smaller than unity. Where, $K=1$ defines the separatrix as the boundary that separates periodic from non-periodic trajectories.

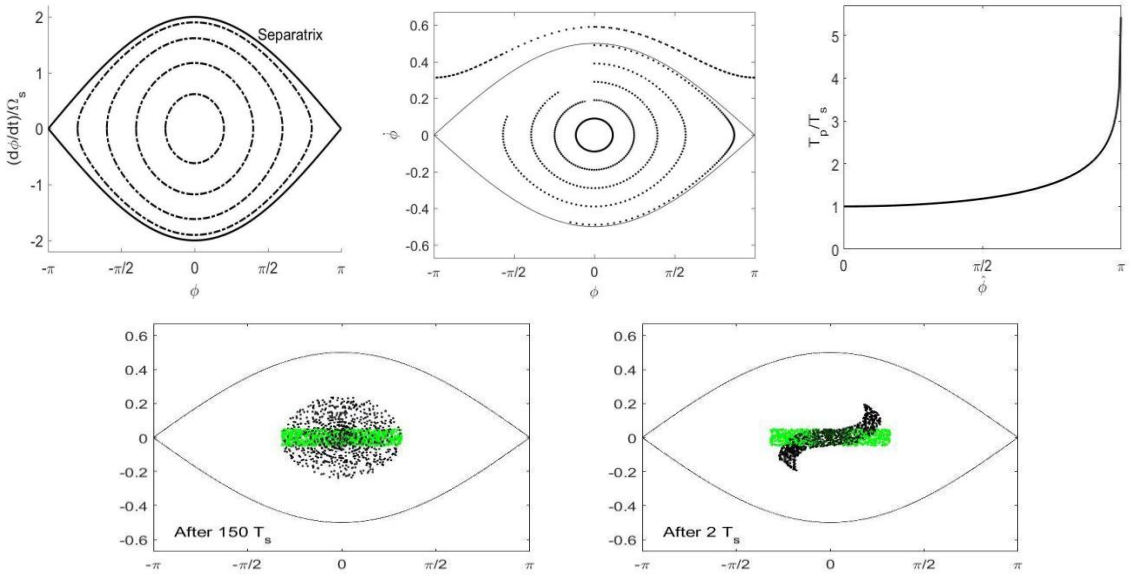

Fig. 3.2.1: Graph (a) represents phase portrait of the longitudinal phase space. Graph (b) oscillation period as a function of the amplitude $\hat{\phi}$. Graph (c) shows trajectories of six particles, starting $\phi = 0$, and $\dot{\phi}$= 0.09, 0.19, 0.29, 0.39, 0.49, and 0.59 for one small amplitude synchrotron period $T_s = \frac{2\pi}{\Omega_s}$. Graphs (d) and (e) respectively show the distribution of 1000 injected particles (green) after two synchrotron oscillation periods and after 150 periods and where a homogeneous/matched distribution emerges.

Hence, (c) is generated by following script for one synchrotron period where particles by 1/100 of one synchrotron oscillation period t_s and plot a dot at every instance. This is repeated for six particles with different starting amplitudes. Plots (d) and (e) are produced by following the script known as longitudinal matching example, which first defines the synchrotron frequency Omegas and synchrotron period t_s. Thus, separatrix is calculated using equation,$\dot{\phi} = \pm 2\Omega_s cos\left(\frac{\phi}{2}\right)$. Here, $x_0 = [0.0,0.0]$ and $dx = [2,0.1]$, then we loop over the N particles. For each particle, select a random position within the box specified by x_0 and dx, and plot a green dot at that point. The pendulum tracker used to map the starting coordinates to those after the desired tracking time and make a black dot at that point.

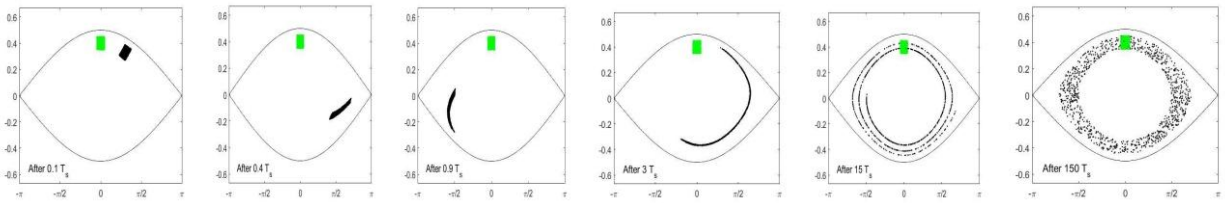

Fig. 3.2.2: Filamentation after injection with too high energy. 1000 particles (green) are followed for up to 150 synchrotron oscillation periods (dark).

In figure 3.2.3 two scripts are used, one is for Landau damping and another for Landau projections. There is apparent damping of averages observed called Landau damping, which is not real damping in the sense that energy is dissipated, but a loss of coherence in the ensemble of particles. Landau projection shows the initial distribution as localized and clustered, and final projections of the distribution with homogenous of particles after $100T_s$. To maintain a small beam size after injection into the ring one has to pay special care to adjust the energy and also the timing, which would lead to the same widening of the distribution. Histograms of both initial and final distributions are produced and displayed on two subplots, each with axes properly annotated.

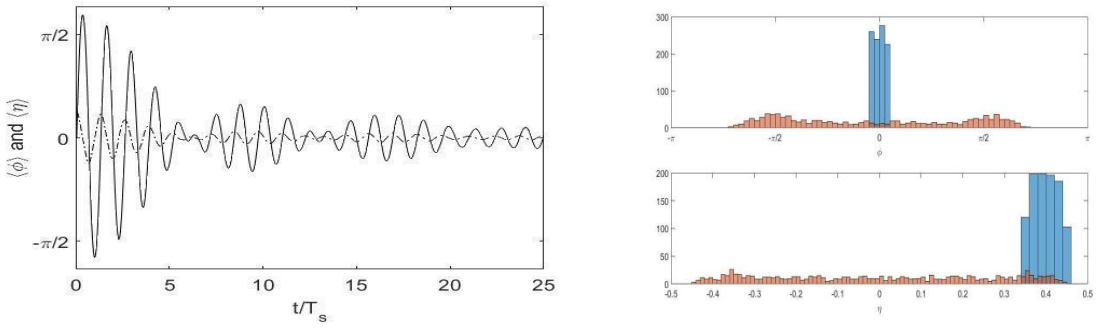

Fig. 3.2.3: The average phase $\langle\phi\rangle$ and energy $\langle\dot{\phi}\rangle$ as a function of time, which shows decoherence, often as landau damping. The projections of the initial distribution and after $100T_s$ for Landau projection.

3.3 Simple LINAC Model

Following the script energy profile for simulation, the first parameters are defined and commented on. Then several arrays are allocated for the phases and energies at every position along the LINAC, where energy-gain of the cavities is defined in array g mentioning broken cavities with reduced gradient. Hence, LINAC must be first phased to adjust the phases to design arrival phase is always equal to the design phase. The known and stored energy profile is then scripted to subdivision into blocks. Here, if 0 … end or 1 … end indicating switch on or off by setting zero to one vice-versa.

If the first block is turned off and the second block is turned on, it generates the schematic representation of the display normal condition. The energy and phase profile for two different initial phases are shown and the third block varies the

arrival phases and displays the achievable final energy. Then, the two blocks vary the energy, first two different energies are explored and lead to the arrival phase while a scan leads to the energy phase. The last block simulates random phase jitter of the cavities and running with two different values of phase max results in the two plots shown in a schematic representation.

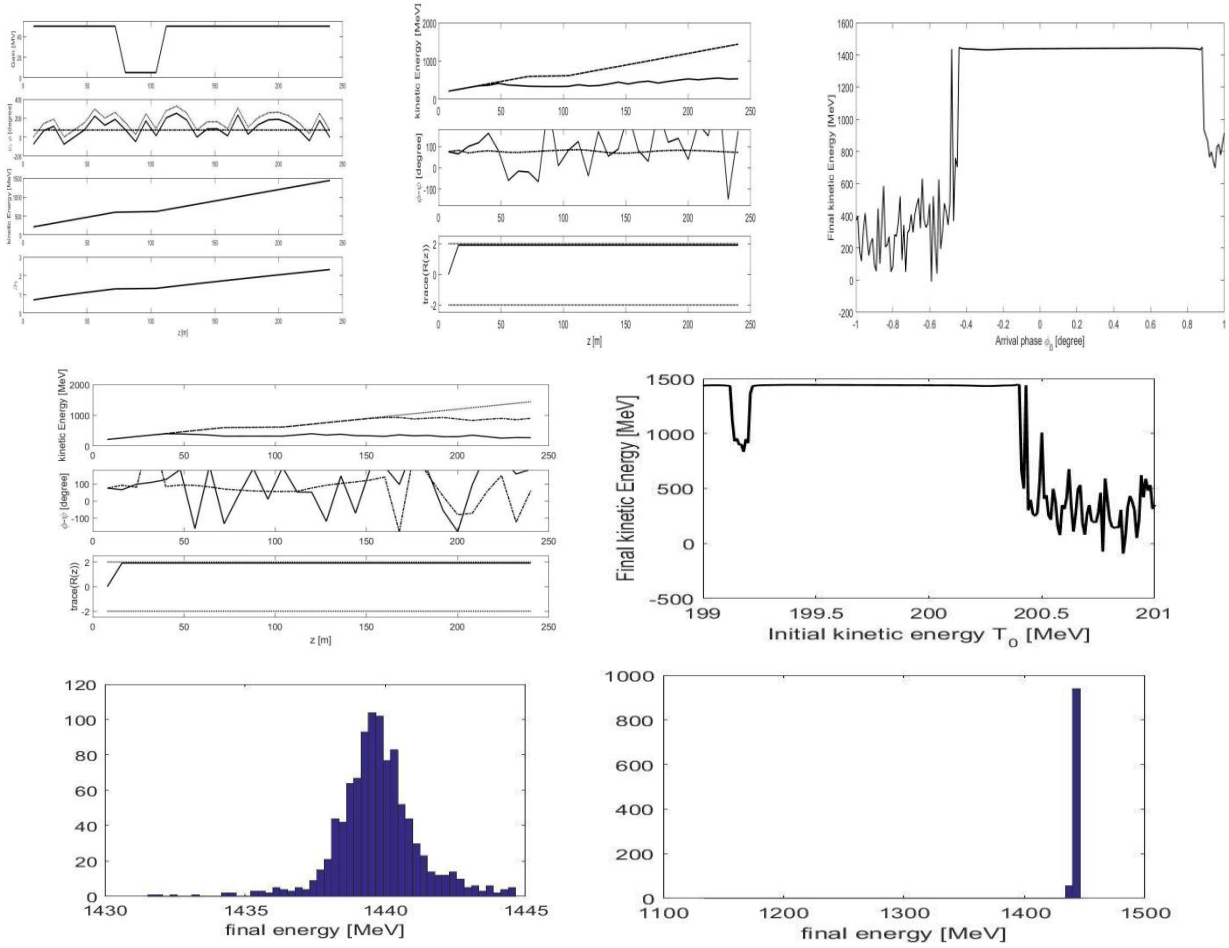

Fig. 3.3.1: Graph (a) shows the energy gain per module (top block), the cavity phases (second block), and energy profile (third block) used to scale the quadrupole excitations. Graphs (b) and (c) represent variation of the initial (arrival) phase $\phi_0 = -0.25$ degree (solid-line) and $\phi_0 = 0.69$ degree (dashes-line). Graphs (d) and (e) shows the final energy(E) as a function of the initial energy(E) with T_0=200.46 MeV (solid-line) and T_0=199.16 MeV (dashes-line). Graphs (f) and (g) represent distribution of final energies for random phase variations of zero degrees (left) and 0.5 degrees (right).

(Note: Graphs a, b, c, d, e, f, and g from above figures of result part count from left to right)

4. CONCLUSION

In this paper we have studied the structure and working procedure of LINAC and have analyzed the energy distribution and instability of particles in phase space. Particle motion is compared with an idealized orbit also we discussed acceleration structure and beam dynamics in LINAC using various technical aspects such as the generation, control power (voltage generator for electric field), and transport. Prodigious output to continuous stream of protons, where a synchrotron was periodically raising the particles to sufficient energy and accelerated particles to a significant fraction of relativistic speed for the production of protons. The application of particle accelerators is constrained to HEP (atom smasher/collider), but the applications are ubiquitous. In HEP, accelerators are vital to study the sub-atomic particles. Other than that, some of the LINACs are used for radiation therapy for cancer treatment and produce medical isotopes utilizing radioactive components like uranium. In industries, they are used to manufacture integrated circuits. Electron beams are also used for sterilization. Similarly, synchrotron

radiations are used in different areas of physics, chemistry, biology to study viable topics, such as beam size estimations, magnet construction, and measurements, and RF measurements are investigated in understudy labs without requiring access to an accelerator. Cockcroft and Walton in 1930 built first particle accelerator with phenomenon called Gamow's tunneling. Smith Lloyd in 1959 studied an idea of producing energetic particles by passing them through a succession of low voltage gaps arranged in a straight line. Alvarez et al., in 1995 described a linear proton accelerator which increases the energy of protons from a 4-Mev Van de Graaff injector to a final energy of 31.5 MeV. In this scrutiny, we found a large amount (100-300 MeV) of energy range of observed and calculated value of energies and comparable phase stability. Thus, different script and schematic representation of longitudinal oscillation, acceleration, and simple LINAC model are verified using MATLAB.

ACKNOWLEDGEMENT

The author expresses sincere gratitude to Mr. Rakesh Chandra Prajapati (ORION Space, Nepal) for assistance with efficient MATLAB coding, who moderated this paper and, in that line, improved the manuscript significantly. The author also extends great appreciation to the CERN Summer Student Programme team for academic consultants.

CONFLICTS OF INTEREST

The authors declare no conflict of interest.

EDITOR'S NOTE

This manuscript was submitted to Association of Nepali Physicists in America (ANPA) Conference 2020 for publication in the special issue of Journal of Nepal Physical Society

REFERENCES

1. Wilson, E. and Wilson; E. J. N. *An introduction to particle accelerators;* Clarendon Press: Oxford, England (2001).
2. Humphries, S. *Principles of charged particle acceleration;* Courier Corporation: Massachusetts, United States (2013).
3. Helmut, W. *Particle Accelerator Physics*, Springer Science & Business Media: Berlin, Germany, 2 (2003).
4. Volker, Z. *Hands-On Accelerator Physics Using MATLAB®;* CRC Press: Florida, United States, 119-137 (2019).
5. Jackson, J. D. *Classical Electrodynamics*, 2nd ed.; Wiley: New York, United States (1975).
6. Griffiths, D. J. *Introduction to electrodynamics*, 4th ed.; Pearson: Massachusetts, United States (2013).
7. Garoby, R. RF Gymnastics in Synchrotrons. CERN Accelerator School, RF for accelerators, Ebeltoft, 431 (2010).